Zahra A W, Ruba A Z, Ahlam M S, Mohammad A Y A, Ahmad Y A, Ahmed M Al-R, Hamza M Al-H, Eman A G, Shereen M A, Zainab M A, Yasser B, Waseem El-H, Karem H A, Mohammad H S. Repurposing Amlodipine for Glioblastoma: A Proteomics study with relevance to pharmacy practice. Pharmacy Practice. 2026 Jan-Marc;24(1):3357.

https://doi.org/10.18549/PharmPract.2026.1.3357

Original Research

Repurposing Amlodipine for Glioblastoma: A Proteomics study with relevance to pharmacy practice

Zahra A. Watad, Ruba A. Zenati, Ahlam M. Semreen, Mohammad A. Y. Alqudah, Ahmad Y. Abuhelwa, Ahmed M. Al-Rawi, Hamza M. Al-Hroub, Eman Abu-Gharbieh, Shereen M. Aleidi, Zainab Al Shareef, Yasser Bustanji, Waseem El-Huneidi, Karem H. Alzoubi, Mohammad H. Semreen

Received: 29-Jul-2025 Accepted: 23-Oct-2025 Published online: 03-Feb-2026

Abstract

Background: Glioblastoma (GBM) is a highly aggressive brain malignancy with limited treatment options due to recurrence, therapy resistance, and invasiveness. Chemotherapy, though essential, is often hindered by severe side effects and chemoresistance. This highlights the need for alternative therapies with reduced cytotoxicity. Recent studies suggest that calcium channel blockers, such as amlodipine, may exhibit anticancer properties across various malignancies. **Objectives:** This study aimed to investigate the molecular changes induced by amlodipine in U87 and U373 GBM cell lines using quantitative proteomics to assess its potential as a repurposed therapeutic agent. **Methods:** Quantitative proteomic analysis was performed using UHPLC-ESI-QTOF-MS on U87 and U373 GBM cell lines treated with amlodipine. Statistical analysis was conducted using a Student's t-test with a q-value < 0.05 to identify significantly dysregulated proteins. **Results:** A total of 1,820 proteins in U87 and 2,250 proteins in U373 were identified. Statistical analysis revealed 77 significantly dysregulated proteins in U87 and 14 in U373. Functional enrichment analysis demonstrated distinct pathway alterations between the two cell lines following amlodipine treatment. In U87 cells, mitochondrial oxidative phosphorylation pathways were deactivated, including NADH dehydrogenase and mitochondrial respiratory chain complex, with significant downregulation of NDUFS1, NDUFS2, and MT-ND4, proteins essential for energy production. In U373 cells, the fluid shear stress and atherosclerosis pathways were activated, with SQSTM1/p62 significantly upregulated. Notably, SQSTM1 was upregulated in both cell lines (4.7-fold in U87 and 2.9-fold in U373), suggesting a potential link between calcium influx inhibition and GBM stress response mechanisms. **Conclusion:** This study provides a comprehensive molecular map of amlodipine-induced proteomic alterations in GBM, highlighting its potential as a repurposed therapeutic agent. The distinct pathway alterations observed between U87 and U373 cell lines underscore the complexity of GBM biology and suggest that calcium channel blockers may exert cell-line-specific effects.

Keywords: Glioblastoma, Amlodipine, Proteomics, Mitochondrial Dysfunction, Drug Repurposing.

Zahra A. Watad. Department of Pharmacy Practice and Pharmacotherapeutics, College of Pharmacy, University of Sharjah, Sharjah 27272, United Arab Emirates. u22105055@sharjah.ac.ae
Ruba A. Zenati. Department of Medicinal Chemistry, College of Pharmacy, University of Sharjah, Sharjah 27272, United Arab Emirates; Research Institute for Medical and Health Sciences, University of Sharjah, Sharjah 27272, United Arab Emirates. u23107609@sharjah.ac.ae
Ahlam M. Semreen. Research Institute for Medical and Health Sciences, University of Sharjah, Sharjah 27272, United Arab Emirates. u21102890@sharjah.ac.ae
Mohammad A. Y. Alqudah. Department of Pharmacy Practice and Pharmacotherapeutics, College of Pharmacy, University of Sharjah, Sharjah 27272, United Arab Emirates; Department of Clinical Pharmacy, Faculty of Pharmacy, Jordan University of Science and Technology, Irbid, 22110, Jordan. malqudah@sharjah.ac.ae
Ahmad Y. Abuhelwa. Research Institute for Medical and Health Sciences, University of Sharjah, Sharjah 27272, United Arab Emirates; Department of Pharmacy Practice and Pharmacotherapeutics, College of Pharmacy, University of Sharjah, Sharjah 27272, United Arab Emirates. ahmad.abuhelwa@sharjah.ac.ae
Ahmed M. Al-Rawi. Research Institute for Medical and Health Sciences, University of Sharjah, Sharjah 27272, United Arab Emirates. u20105592@sharjah.ac.ae
Hamza M. Al-Hroub, Research Institute for Medical and Health Sciences, University of Sharjah, Sharjah 27272, United Arab Emirates. halhroub@sharjah.ac.ae
Eman Abu Gharbiah. Research Institute for Medical and Health Sciences, University of Sharjah, Sharjah 27272, United Arab Emirates; Department of Clinical Sciences, College of Medicine, University of Sharjah, Sharjah 27272, United Arab Emirate; Department of Biopharmaceutics and Clinical Pharmacy, School of Pharmacy, The University of Jordan, Amman 11942, Jordan. eabugharbieh@sharjah.ac.ae
Shereen M. Aleidi. Department of Medicinal Chemistry, College of Pharmacy, University of Sharjah, Sharjah 27272, United Arab Emirates; Research Institute for Medical and Health Sciences, University of Sharjah, Sharjah 27272, United Arab Emirates; Department of Biopharmaceutics and Clinical Pharmacy, School of Pharmacy, The University of Jordan, Amman 11942, Jordan. saleidi@sharjah.ac.ae
Zainab M. AlShareef. Research Institute for Medical and Health Sciences, University of Sharjah, Sharjah 27272, United Arab Emirates; Department of Basic Medical Sciences, College of Medicine, University of Sharjah, Sharjah 27272, United Arab Emirates. zalshareef@sharjah.ac.ae
Yasser Bustanji. Research Institute for Medical and Health Sciences, University of Sharjah, Sharjah 27272, United Arab Emirates; Department of Biopharmaceutics and Clinical Pharmacy, School of Pharmacy, The University of Jordan, Amman 11942, Jordan; Department of Basic Medical Sciences, College of Medicine, University of Sharjah, Sharjah

www.pharmacypractice.org (eISSN: 1886-3655 ISSN: 1885-642X)

https://doi.org/10.18549/PharmPract.2026.1.3357

27272, United Arab Emirates. ybustanji@sharjah.ac.ae
Waseem El-Huneidi. Research Institute for Medical and Health Sciences, University of Sharjah, Sharjah 27272, United Arab Emirates; Department of Basic Medical Sciences, College of Medicine, University of Sharjah, Sharjah 27272, United Arab Emirates. welhuneidi@sharjah.ac.ae
Karem H. Alzoubi*. Research Institute for Medical and Health Sciences, University of Sharjah, Sharjah 27272, United Arab Emirates; Department of Pharmacy Practice and Pharmacotherapeutics, College of Pharmacy, University of Sharjah, Sharjah 27272, United Arab Emirates. kelzubi@sharjah.ac.ae
Mohammad H. Semreen*. Department of Medicinal Chemistry, College of Pharmacy, University of Sharjah, Sharjah 27272, United Arab Emirates; Research Institute for Medical and Health Sciences, University of Sharjah, Sharjah 27272, United Arab Emirates. msemreen@sharjah.ac.ae

INTRODUCTION

Glioblastoma (GBM) is one of the devastating cancers, accounting for more than 60% of the brain cancers in adults[1] and 3% of brain cancers in the paediatric population[2]. Over the past 30 years, immense efforts and resources have been invested in drug discovery research area aiming to find a long-term effective therapeutic approach that could enhance clinical outcomes, increase the survival rates and lower the risk of recurrence[2,3]. Despite the advances in brain cancers research, still the survival rate in most patient is short and barely exceeds 12 months, with less than 5% of patients survive for more than 5 years[3,4]. In elderly patients, this percentage decreases to around 2%[3]. About 90-95% of GBM patients have cancer recurrence about 2cm from the primary cancer[5]. GBM represents a highly challenging cancer to treat due to several factors. The cancer's localization within the central nervous system and being protected by the blood-brain barrier (BBB)[6], which functions as a selective permeability barrier expressing efflux pumps that actively eliminate potentially cytotoxic agents[7]. Furthermore, the heterogeneity of GBM promotes therapeutic resistance by facilitating the selection and expansion of resistant subpopulations[8]. These biological and anatomical complexities collectively impede the efficacy of conventional chemotherapeutic treatment modalities.

Understanding the molecular pathophysiology of GBM would provide significant potential for identifying novel therapeutic targets that can be integrated with current standard-of-care modalities, including surgical resection, radiotherapy, and chemotherapy[9]. These multimodal approaches can be optimized to achieve synergistic effects, such as cancer debulking through surgical intervention, angiogenesis inhibition to disrupt the cancer's vascular supply and nutrient acquisition[9], and targeting dysregulated molecular pathways and aberrant protein expression through precision therapeutics[10,11]. Due to the substantial economic burden of GBM, with treatment costs reaching up to $95,000 per patient [12], its high global incidence of approximately 300,000 cases annually[13], and the protracted and resource-intensive nature of new drug discovery , drug repurposing approach represents an efficient strategy that accelerates the identification of efficacious therapeutic agents for GBM[14].

Amlodipine, a calcium channel blocker primarily prescribed for hypertension and other cardiovascular conditions[15], has shown promise in this context. Recent studies on repurposing FDA-approved drugs aim to reduce the time and cost of cancer treatments. Amlodipine has demonstrated anticancer properties[16], particularly in breast cancer cell lines such as MDA-MB-231 and MCF-7. It inhibits proliferation and growth by activating caspase-3/7, key mediators of apoptosis, and further impedes breast cancer cell invasion and proliferation[17]. In lung cancer cell lines, amlodipine was combined with chemotherapeutic carboplatin, gemcitabine, pemetrexed, or paclitaxel, and it significantly sensitized A549 and H1299 non-small cell lung cancer (NSCLC) cells compared to their single-drug treatments[18]. Additionally, when combined with gefitinib in NSCLC, amlodipine suppresses critical molecular pathways such as PI3K/Akt and Raf/MEK/ERK through epidermal growth factor receptor (EGFR) modulation and regulates cell cycle-related proteins, including cyclin D1, p-Rb, p27, and p2[19]. Integrating multi-omics approaches, including genomics, proteomics, transcriptomics, and metabolomics, has profoundly advanced cancer research[20,21]. These high-throughput methods provide comprehensive molecular insights that can be utilized to identify clinical subtypes, study drug resistance patterns, predict treatment responses, and discover novel biomarkers and therapeutic targets within the heterogeneous cancer microenvironment [22, 23]. Among these approaches, proteomics holds promise by examining the changes in proteins, the functional end products of genes. Given that cancer is fundamentally a genetic disease marked by diverse mutations, proteomics reflects the resultant alterations at the protein level. This field enables the identification of potential biomarkers and the assessment of treatment impacts on specific proteins or pathways [24].

In our study, we aimed to explore one of the most treatment-resistant cancers, GBM, through proteomics. By identifying new potential biomarkers and evaluating the impact of repurposed drugs such as amlodipine, we sought to determine whether this drug modulates the expression of specific proteins. The integration of proteomic insights with drug repurposing strategies like those demonstrated for amlodipine offers a promising avenue for overcoming therapeutic challenges in GBM and potentially enhancing treatment efficacy.

MATERIALS AND METHODS

Reagents

Formic acid (FA) from Fisher Chemical (Loughborough, UK), Methanol ≥ 99.9 % LC-MS CHROMASOLV, Deionized Water, and acetonitrile (ACN) LC-MS CHROMASOLV from Honeywell (Seelze, Germany), Pierce Protease inhibitor, Lysis buffer (Catalog number: 87787), and C18 tips from Thermoscientific (Rockford, USA), Bovine Serum Albumin and Bradford's reagent from Sigma-Aldrich (Louis, USA), Hydrochloric acid (HCl) 37 %

from VWR chemicals (France), and Pirece Trypsin Protease and Lysyl Endopeptidase LysC from Thermoscientific (Rockford, USA).

Cell line and culture conditions

Two distinct GBM cell lines (U87 and U373) were used. These two cell lines represent different phenotypes of GBM. U373 cell line represents slow-proliferating cells, whereas U87 is considered a rapidly proliferating cell line. Both cell lines differ in their genetic expression profile. U87 expresses phenotypes that are like neuronal, while U373 expresses mesenchymal characteristics[25]. Two million cells were seeded into T75 cell culture flasks and incubated overnight. Control cells were treated with 0.5% Dimethyl sulfoxide (DMSO) for 24h. Both cell lines (U87 and U373) were treated with amlodipine at a concentration of 24 µM for 24 hours. This concentration was selected based on IC_{50} values obtained from preliminary data of unpublished research. After incubation, the cells were harvested by trypsinization, washed twice with PBS, and resuspended in 1ml of PBS. Subsequently, the cells were centrifuged at 1200rpm for 10 min at room temperature and the resultant pellets were collected. The resultant four groups with five biological replicates were stored at – 80 °C for subsequent proteomic analyses.

Protein Extraction

The used protocol is a well-established and known for its high efficiency in achieving broad protein coverage during extraction[26]. Briefly, frozen cell pellets from the respective treatments were thawed and spun at 14000 rpm, 25 °C for 5 min to separate the cells from the PBS buffer. Then, the pellets were subjected to 400 µL of lysis buffer. The samples were then ultrasonicated to destroy insoluble matrices. The remaining cell debris was removed after the samples were centrifuged at 14000 rpm for 5 min, whereby the supernatants were transferred to Eppendorf tubes. Next, 400 µL of methanol, followed by 300 µL of chloroform, were added to the samples and vortexed to mix the resultant solution. After that, they were centrifuged at 14000 rpm, 25 °C for 5 min, which yielded two layers and a protein-rich disc at the interphase. The biphasic aqueous layers were discarded while protein pellets were air dried for 10 min. Samples subsequently reconstituted in 100µl denaturation buffer consisting of 6 M urea and 2 M thiourea in 10 mM tris(hydroxymethyl) aminomethane (tris) buffer (pH 8). Protein quantification and digestion were performed using a modified Bradford assay and in-solution digestion, respectively.

100 µg of Dithiothreitol was used to for reduction and breaking the disulfide bonds, which were then incubated for an hour at room temperature (RT) with agitation at 100 rpm. Samples were then alkylated with iodoacetamide (5.5 mM) and incubated for 1h at 100 rpm in the dark. For protein digestion, 1 µg of Lys-C (1:100 w/w) was added to the samples, followed by incubation at RT for 3 hours at 100 rpm. The samples were then diluted fourfold with 20 mM ammonium bicarbonate and further digested with 1 µg of trypsin (1:100 w/w). Digestion was carried out overnight at RT with gentle shaking at 100 rpm. Next, the samples were dried, resuspended in 1% trifluoroacetic acid, and filtered using C18 stage tips for desalting[37]. Peptides were eluted into LC vials after aspiration and dispensing 100 µL of 0.1 % formic acid (FA) in 60 % acetonitrile (ACN). The eluted peptides were subsequently dried with and resuspended in 100 µL of 0.1 % FA in 2 % ACN for LC-MS/MS analysis.

LC-MS/MS conditions

The LC-MS/MS analysis was carried out using a nano elute system (Bruker Daltonics) coupled with a quadrupole-time-of-flight mass spectrometer (Q-TOF), equipped with a Captive-Spray ion source (Bruker Daltonics). Utilizing a sample volume of 4 µL (equivalent to 4 µg of peptides), separation took place over a 140 min gradient using solvent A (0.1 % formic acid in deionized water) and solvent B (0.1 % formic acid in acetonitrile) according to the following profile: 0 to 5 min, 5 % B; 5 to 120 min, 5–35 % B; 120 to 125 min, 35 to 95 % B; 125 to 135 min, 95 % B; 135 to 135.2 min, 95–5 % B; 135.2–140 min, 5 % B. The flow rate was maintained at 0.30 µL per minute, and the Captive-Spray ion source operated at 3.0 L/min and 150 °C. The capillary voltage was set at 1600 V. Auto MS/MS scans using CID acquisition were employed in positive mode at 2 Hz. During the automatic in-run mass scan, the mass analysis covered a range from 150 to 2200 m/z, with a precursor width of 0.5, two precursors, a cycle time of 3.0 s, and a threshold of 500 cts. Exclusion was triggered after 1 spectrum and released after 2.0 minutes. MS2 acquisition utilized data-dependent acquisition (DDA), and the collision energy was adjusted within the range of 23–65 eV based on m/z.

Western blot analysis

After cell lysis, protein extraction was performed using a M-PER™ Mammalian Protein Extraction Reagent (Thermo Scientific, 78501), and the protein was estimated using Bradford reagent (Bio-Rad – 500-0006). Total protein samples were loaded at 25 µg/well onto a sodium dodecyl sulfate-polyacrylamide gel (SDS-PAGE) for electrophoresis. Subsequently the separated proteins were transferred to PVDF membrane (Bio-Rad 1620177) using a semi-dry transferring method. The membranes were incubated in a 5% BSA solution at RT for one hour. Then, the membranes were treated with primary antibodies against ECEL1 (1:500, ab228490, Abcam), SQSTM1/p26 (1:1000, ab109012, Abcam), IMPAD1 (1:500, ab69311, Abcam), SCD (1:500, A16429, Abclonal), TOP2A (1:2000, 24641-1-AP, Proteintech), and the loading control GAPDH (1:1000, ab8245, Abcam). The primary antibodies were incubated overnight at 4 °C, followed by washing with TBS-T. The, the membranes were incubated with with secondary antibodies, either anti-rabbit IgG horse radish peroxidase (HRP)-linked Antibody (#7074, Cell signaling) or Anti-mouse IgG HRP-linked Antibody (#7076, Cell signaling), according to the type of the used primary antibodies. The secondary antibodies were incubated at RT for 90 minutes followed by washing with TBS-T. The Bio-Rad Chemi-Doc gel imaging equipment was used to detect the protein bands and ImageJ software was used to measure the band density. To ensure the reliability of the findings, all experiments were performed in triplicate, with independent repeats conducted three times.

https://doi.org/10.18549/PharmPract.2026.1.3357

Bioinformatics analysis and statistical approach

To identify the proteins and peptides, the raw data were processed using MaxQuant (version 1.6.17.0) software (https://www.maxquant.org/) using the UniProt proteome for homo sapiens (Proteome iD: UP000005640, 81,791 entries) and the andromeda search engine. In the MS/MS database search, default parameters were used, including variable modifications, such as methionine oxidation and acetylation of protein N-termini, and fixed modifications, such as carbamidomethylation of cysteine residues. Peptide spectral matching (PsMs) was performed using a 20-ppm precursor mass tolerance and a 1% false discovery rate (FDR). The MaxLFQ algorithm was used for label-free quantification (LFQ). The default trypsin/P enzymatic cleavage rule was used for in-silico digestion. The data were filtered to remove potential contaminant proteins and proteins solely recognized by the site and reverse proteins. LFQ data were transformed into $\log_2$ (x). Proteins were annotated and those with 70% valid values were used for further analysis. To determine the substantially expressed proteins in treated and untreated U87 and U373 cells, a two-tailed independent student's t-test was used. A fold change threshold of ±1.4 and *p-value < 0.05* were applied to identify differentially expressed features. The choice of ±1.4 FC cutoff was selected based on its frequent use in high-throughput omics studies which reflect biologically meaningful differences. To account for multiple hypothesis testing, the Benjamini-Hochberg false discovery rate (FDR) correction was applied. Proteins meeting the criteria of adjusted *p < 0.05* and FC ≥ ±1.4 were considered statistically significant. To evaluate the expression of differentially expressed proteins in each group and to show group clustering, hierarchical clustering and a heat map were generated. More importantly, dysregulated proteins with an adjusted *p-value* < 0.05 were examined for enrichment by the Gene set enrichment analysis (GSEA) through R software programming to display the gene ontology (GO) keywords for biological processes. Venn diagram was generated by using Bioinformatics and Evolutionary Genomics (http://bioinformatics.psb.ugent.be/webtools/Venn/ (accessed on 10 January 2025), and protein-protein interaction network analysis was dose using STRING.

RESULTS

Proteomic profiling of the brain cancer cell lines after treatment with Amlodipine

In this study, LC-MS/MS has been utilized to perform proteomics analysis on two brain cancer cell lines U87 and U373 treated with the antihypertensive calcium channels blocker amlodipine. In our comparative proteomic analysis, 1,820 and 2,250 proteins were identified in the U87 and U373, respectively. In the U87 cell line, the Principal Component analysis (PCA), showed a separation between the control and treated groups indicating high response to the treatment (Figure 1A). However, in U373, there was an overlap between the control and the treatment groups, indicating a lower response towards the treatment (Figure 1B). By conducting a student's t-test with a *q-value* < 0.05, the results showed 77 significantly dysregulated proteins in the U87 cell line, whereas U373 had only 14 significant proteins (Supplementary Table S1). The hierarchical clustering heatmaps illustrate the significantly dysregulated proteins in U87 and U373 glioblastoma cell lines following amlodipine treatment. In U87 cells, a distinct separation between treated and control groups is observed, with pronounced differences in protein expression profiles, indicating a robust effect of amlodipine (Figure 2A). Similarly, in U373 cells, the heatmap depicts a clear differentiation between treated and control groups (Figure 2B). To further characterize these proteomic changes, volcano plots were generated for both cell lines, illustrating the differential protein abundance following amlodipine treatment. In U87 cells, among the significantly dysregulated proteins (n=77), 20 were upregulated and 57 were downregulated (Figure 3A). In U373 cells, among the significantly dysregulated proteins (n = 14), 9 were upregulated and 5 were downregulated (Figure 3B). The greater number of dysregulated proteins in U87 suggests a more pronounced proteomic response to amlodipine compared to U373. These findings align with our PCA analysis, where U87 exhibited clear separation between treated and control groups, whereas U373 showed an overlap, indicating a relatively lower molecular response to the treatment. Amlodipine treatment also resulted in distinct protein dysregulation patterns between the two cell lines, as illustrated in the Venn diagram (Figure 3C).

A total of 72 proteins were significantly dysregulated exclusively in U87, while 9 were unique to U373. Additionally, 5 proteins were commonly dysregulated in both cell lines. These findings indicate distinct proteomic changes following amlodipine treatment, with a greater number of differentially expressed proteins observed in U87 compared to U373. These findings suggest that while U87 cells exhibit a more pronounced global proteomic response to amlodipine, U373 cells still display specific protein-level changes, underscoring the heterogeneous nature of GBM and its differential sensitivity to calcium channel inhibition.

Protein expression analysis of significantly dysregulated proteins in the brain cancer cell lines treated with Amlodipine

In order to validate the findings of our proteomic analysis, western blot analysis was conducted to confirm the expression levels of selected dysregulated proteins (Figure 4). The selection of proteins for validation was based on their significant dysregulation and biological relevance in both U87 and U373 glioblastoma cell lines. SQSTM1 and FDFT1 were chosen as they were significantly upregulated in both cell lines, aligning with our proteomic results. Specifically, SQSTM1 expression increased by 4.7-fold in U87 and 2.9-fold in U373, while FDFT1 showed a 2.2-fold increase in U87 and a 3.2-fold increase in U373 following amlodipine treatment. Furthermore, ECE1 was downregulated by 2-fold, SCD was upregulated by 8.2-fold, and IMPAD1 was downregulated by 1.9-fold, all of which were confirmed by western blot analysis (Figure 4A and B). Additionally, TOP2A was selected due to its 2-fold downregulation in U373, which was consistent with western blot results (Figure 4C and D).

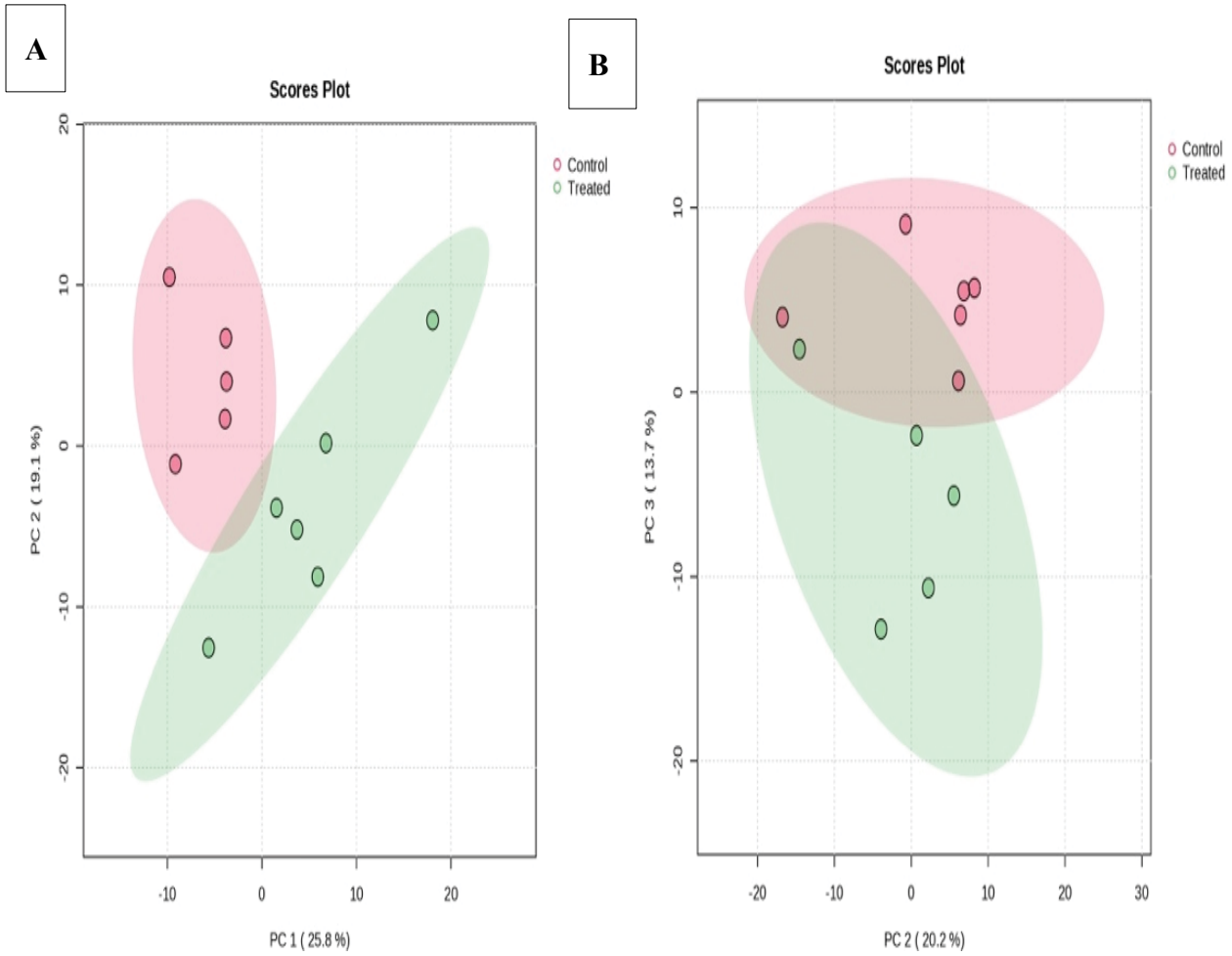

Figure 1. Proteomics profiling of the brain cancer cell lines. PCA between control and treated cells in (A) U87 and (B) U373 cell lines.

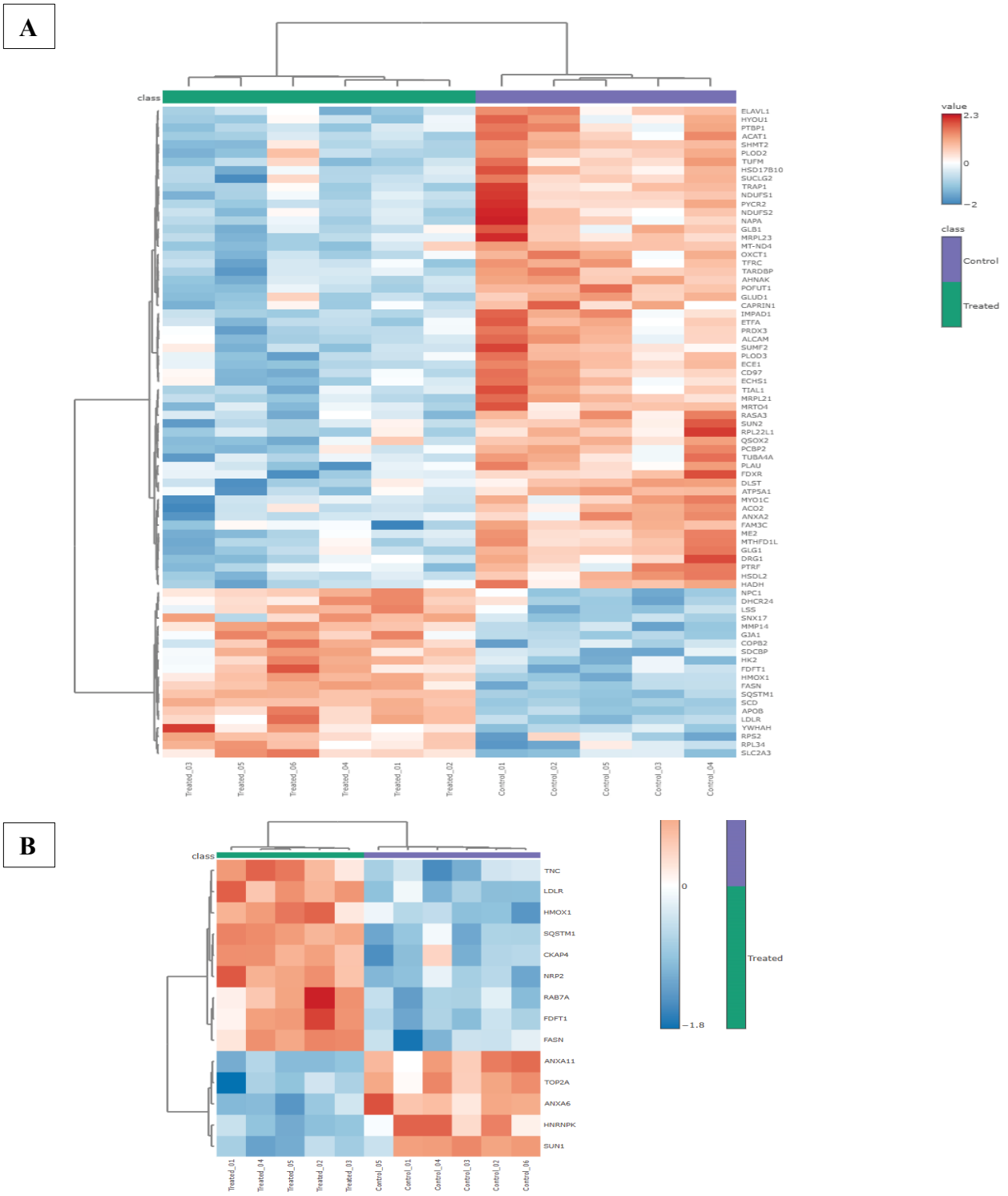

Figure 2. Hierarchical clustering heatmaps of significantly dysregulated expressed proteins in glioblastoma cell lines following amlodipine treatment. (A) U87 cell line and (B) U373 cell line. The heatmaps illustrate hierarchical clustering of protein expression levels in control and treated groups. The colour scale represents the expression levels, where red indicates upregulation, blue indicates downregulation, and intermediate colours reflect moderate changes. Proteins are listed on the right, while the sample groups are indicated on the x-axis.

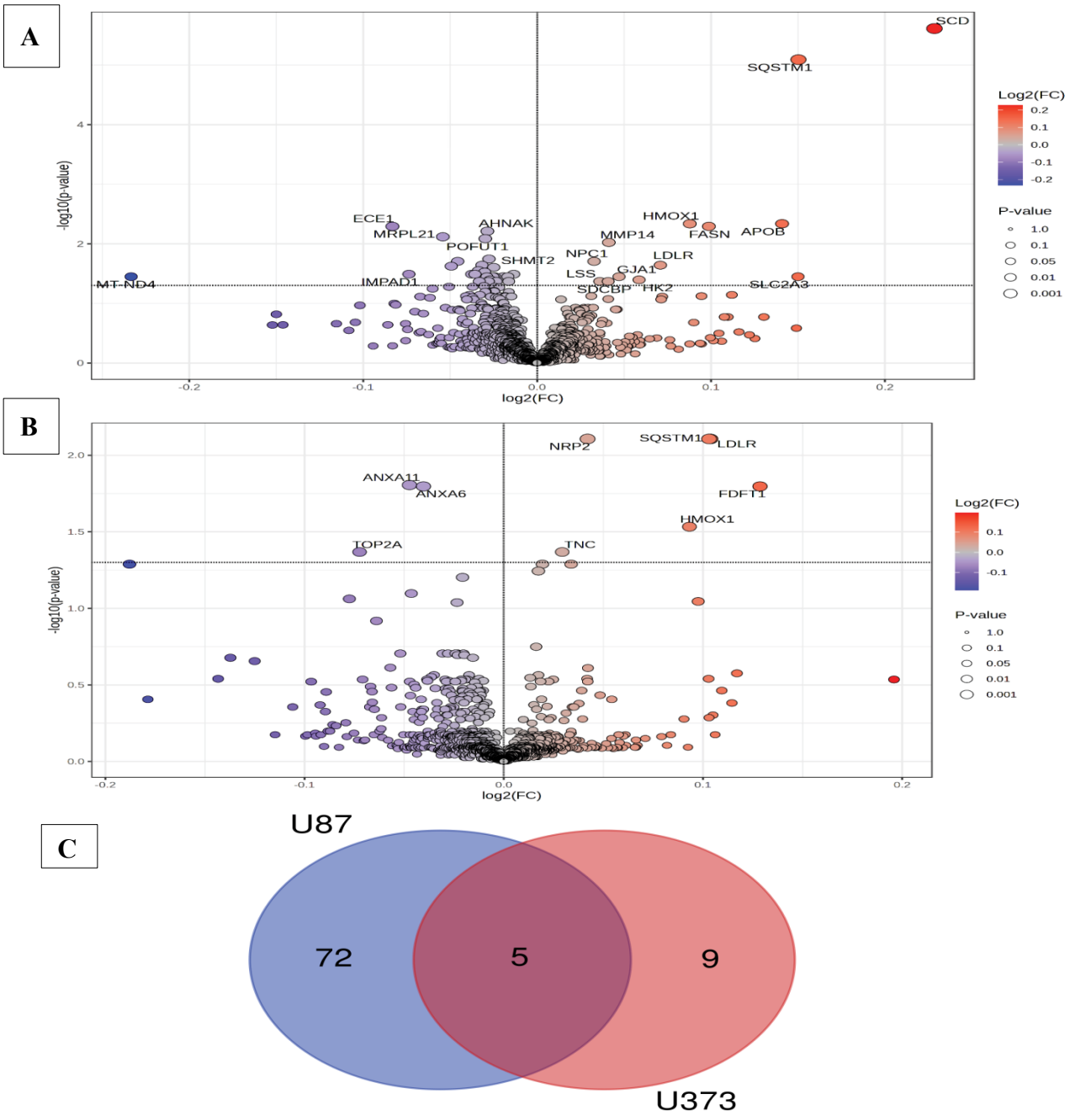

Figure 3. Differentially expressed proteins in U87 and U373 glioblastoma cell lines following amlodipine treatment. (A, and B) Volcano plots illustrating the differentially expressed proteins in glioblastoma cell lines following amlodipine treatment. (A) U87 cell line and (B) U373 cell line. The x-axis represents the log2 fold change (FC) of protein expression, while the y-axis represents the log10(p-value). Upregulated proteins in treated cells are depicted in red, downregulated proteins in blue, and non-significant proteins in black. The size of the data points corresponds to the significance level, with larger circles indicating lower p-value. (C) Venn diagram illustrating the overlap of significantly dysregulated proteins between U87 and U373 glioblastoma cell lines following amlodipine treatment.

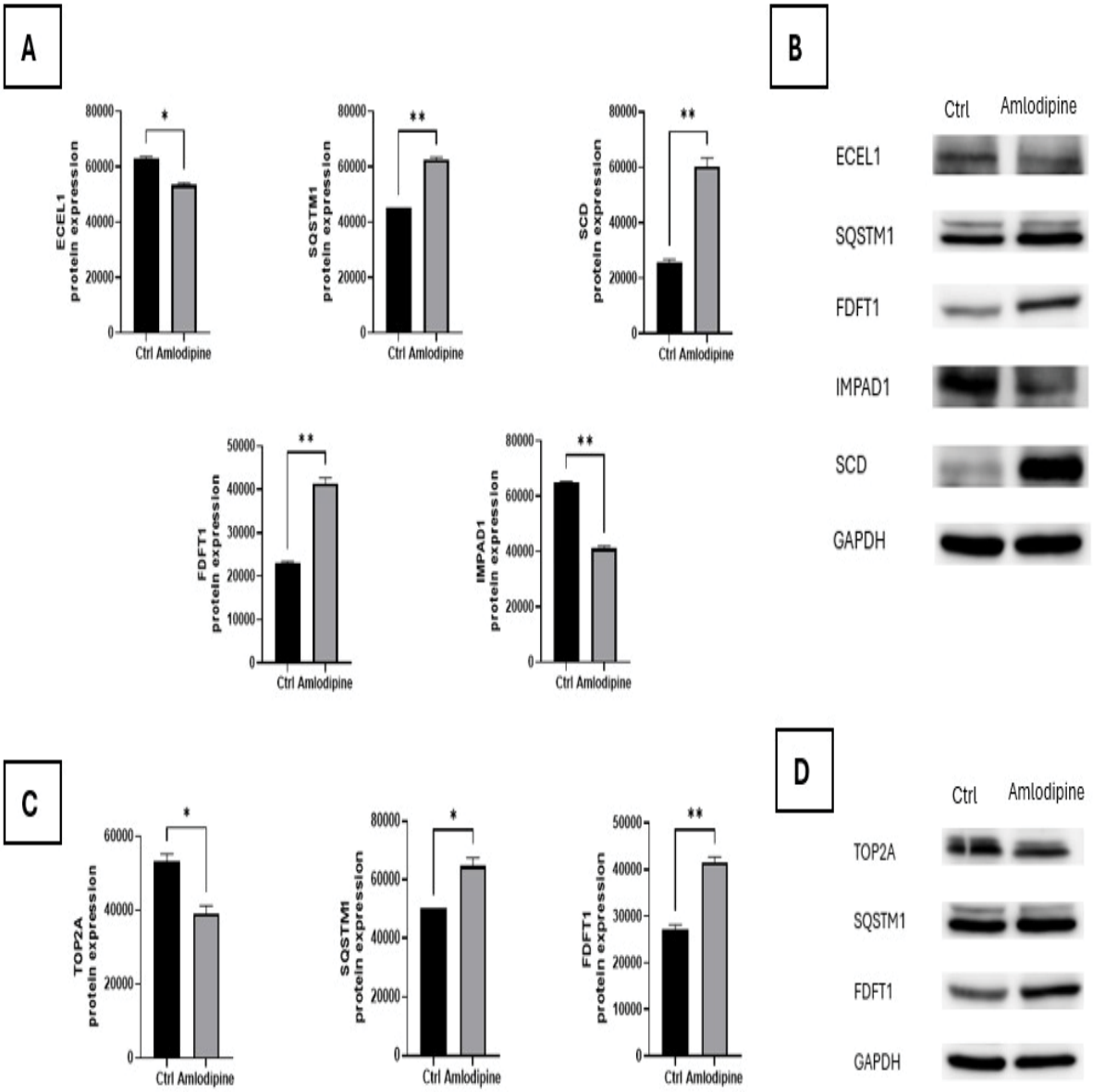

Figure 4. Protein expression analysis in U87 and U373 cell lines treated with amlodipine. Quantitative expression levels of key proteins, including ECEL1, SQSTM1, SCD, FDFT1, and IMPAD1, in the U87 cell line are shown in (A), with significant alterations observed following amlodipine treatment compared to the control (Ctrl). Representative Western blot images for these proteins in the U87 cell line are presented in (B). Similarly, quantitative expression levels of proteins TOP2A, SQSTM1, and FDFT1 in the U373 cell line are displayed in (C), highlighting significant differences between amlodipine-treated and control groups. Corresponding Western blot images for these proteins in the U373 cell line are shown in (D). GAPDH was used as the loading control for both cell lines. Statistical significance is indicated as *$p < 0.05$ and **$p < 0.01$, with error bars represent the standard deviation (SD) from three independent biological replicates.

Pathways analysis of the significantly dysregulated proteins in the brain cancer cell lines treated with Amlodipine

After identifying the significantly dysregulated proteins, gene set enrichment analysis (GSEA) was performed to identify enriched pathways, offering deeper insights into the biological functions and mechanisms underlying the observed changes in protein expression. Gene sets utilized in GSEA were derived from functional annotations of proteins provided by pathway databases such as the Kyoto Encyclopedia of Genes and Genomes (KEGG), Reactome, and Gene Ontology (GO). These gene sets represent functionally related groups of proteins involved in distinct biological processes or pathways. Significantly dysregulated proteins were used as input for GSEA analysis, which determines whether each gene set is activated (normalized enrichment score (NES) > 0) or deactivated (NES < 0). Our enrichment analysis revealed that, in the U87 cell line, only two pathways were activated: Coronavirus disease - COVID-19 and fluid shear stress and atherosclerosis.

On the other hand, majority of pathways including transporter complex, transmembrane transporter complex, respiratory chain complex, oxidoreductase complex, NADH dehydrogenase complex, mitochondrial respiratory chain complex, and diabetic cardiomyopathy were deactivated (Figure 5A). In contrast, based in the dysregulated proteins in the U373 cell line only one pathway was found to be activated pathway. This pathway was fluid shear stress and atherosclerosis, with no deactivated pathways observed (Figure 5B). Interestingly, the fluid shear stress and atherosclerosis was activated in both cell lines indicated that this pathway might be related to the GBD pathophysiology and might be affected upon amlodipine treatment. Additionally, the protein-protein interaction network analysis highlights the differential proteomic response of U87 and U373 GBM cell lines following amlodipine treatment (Figure 5C). Proteins significantly dysregulated in U87 were primarily clustered within a highly interconnected network, suggesting widespread proteomic alterations. In contrast, U373-specific dysregulated proteins exhibited a more dispersed pattern, indicating a more targeted response. A subset of proteins including (SQSTM1, FDFT1, HMOX1, LDLR, and FASN) were commonly dysregulated in both cell lines, representing potential shared molecular pathways influenced by amlodipine. The differences in network topology suggest that U87 cells experience broader proteomic shifts, whereas U373 cells exhibit a more specific adaptive response. The proteins significantly dysregulated and enriched in these pathways are summarized in Table 1.

DISCUSSION

Calcium is a crucial ion in the human body. It has several integral roles in many physiological processes. Maintaining calcium homeostasis is essential, and any disruption can lead to a range of diseases. The regulation of calcium levels is mediated by numerous channels and receptors distributed throughout the body. In the brain, calcium signalling is a key driver of glial cell invasion and migration, significantly contributing to glioma progression. Several types of calcium channels regulate intracellular calcium signaling, including inositol 1,4,5-triphosphate receptors (IP3Rs), store-operated channels (SOCs), transient receptor potential (TRP) channels, voltage-gated calcium channels (VGCCs), P2X7 receptors, and ionotropic glutamate receptors. These pathways collectively influence the motility and invasive properties of glioma cells[33]. Extensive research has been conducted on the role of calcium channel alterations in the metastasis and invasion of GBM, with particular emphasis on VGCCs. VGCCs are classified into high voltage-activated channels (P/Q, N-, and L-types), intermediate voltage-activated channels (R-type), and low voltage-activated channels (T-types). Studies have demonstrated that blocking T-type VGCCs using endostatin significantly reduces glial cell proliferation and migration[34]. Similarly, the inhibition of P/Q- and N-type VGCCs has been shown to suppress glioma growth both *in vivo* and *in vitro* by impairing cellular proliferation[33,35]. However, there is no sufficient data available on the consequences of knockdown of L-type VGCCs.

In this context, the present study investigates the potential of amlodipine, an antihypertensive drug primarily targeting L-type VGCCs, as a repurposed therapeutic agent against GBM. Amlodipine has demonstrated anticancer properties in other cancer types, but its impact on GBM has not been fully elucidated. This study provides significant insights into the molecular changes induced by amlodipine in GBM cell lines U87 and U373. The proteomic analysis revealed a difference in the response of the two cell lines to amlodipine treatment. In the U87 cell line, 77 proteins were identified as significantly dysregulated, whereas the U373 cell line displayed 14 significantly dysregulated proteins. This disparity underscores the heterogeneity of GBM and highlights the distinct molecular and phenotypic characteristics of these cell lines, where U87 exhibits rapid proliferation and neuronal-like phenotypes, while U373 represents slower proliferating mesenchymal-like cells. Among the significantly dysregulated proteins identified, four were particularly noteworthy due to their established roles in GBM biology: MT-ND4, NDUFS1, NDUFS2, and SQSTM1/p62. These proteins are centrally involved in mitochondrial respiration, energy metabolism, autophagy, and tumor cell survival. Their altered expression patterns in response to amlodipine treatment suggest that the drug may interfere with key oncogenic pathways in GBM. One of the key dysregulated pathways in U87 cells involves mitochondrial function, which plays a crucial role in maintaining cellular bioenergetics. Specifically, NADH dehydrogenase complex, mitochondrial respiratory chain complex, oxidative phosphorylation, and oxidoreductase complex. These pathways are integral to ATP production and energy metabolism, and their disruption can significantly impair cancer cell survival and proliferation.

Mitochondria serve as the powerhouse of the cell, producing ATP through oxidative phosphorylation, a process that is upregulated in many cancers to meet the high energy demands required for cancer growth, proliferation, and metastasis[36]. Oxidative phosphorylation relies on the activity of NADH and FADH2to reduce oxygen and generate ATP[37,38]. Recent studies in colorectal cancer and precancerous adenomas have identified NDUFS1, a key mitochondrial complex I subunit, as a binding partner to Prohibitin 2 (PHB2), where their interaction enhances oxidative phosphorylation, thereby promoting cancer progression[30]. In our study, amlodipine treatment led to a 1.4-fold decrease in NDUFS1 expression compared to the control, further supporting the drug's potential impact on glioma cells by disrupting mitochondrial function.

Additionally, research in pancreatic cancer has shown that NDUFS2, another complex I subunit, plays a key role in activating the PI3K/Akt pathway, which enhances cancer proliferation, migration, and metastasis through its interaction with NUDT21 (Nudix Hydrolase 21) that has been found to play a dual role by being cancer suppressor and an oncogene[39]. Interestingly, previous studies have reported that NUDT21 expression is decreased in GBM[40]. Given that NDUFS2 is associated with multiple cellular functions, its disruption leads to reduced cell growth and impaired complex I-specific respiration, which is crucial for energy production[41]. Furthermore, the loss of NDUFS2 has been linked to an increase in complex II respiration,

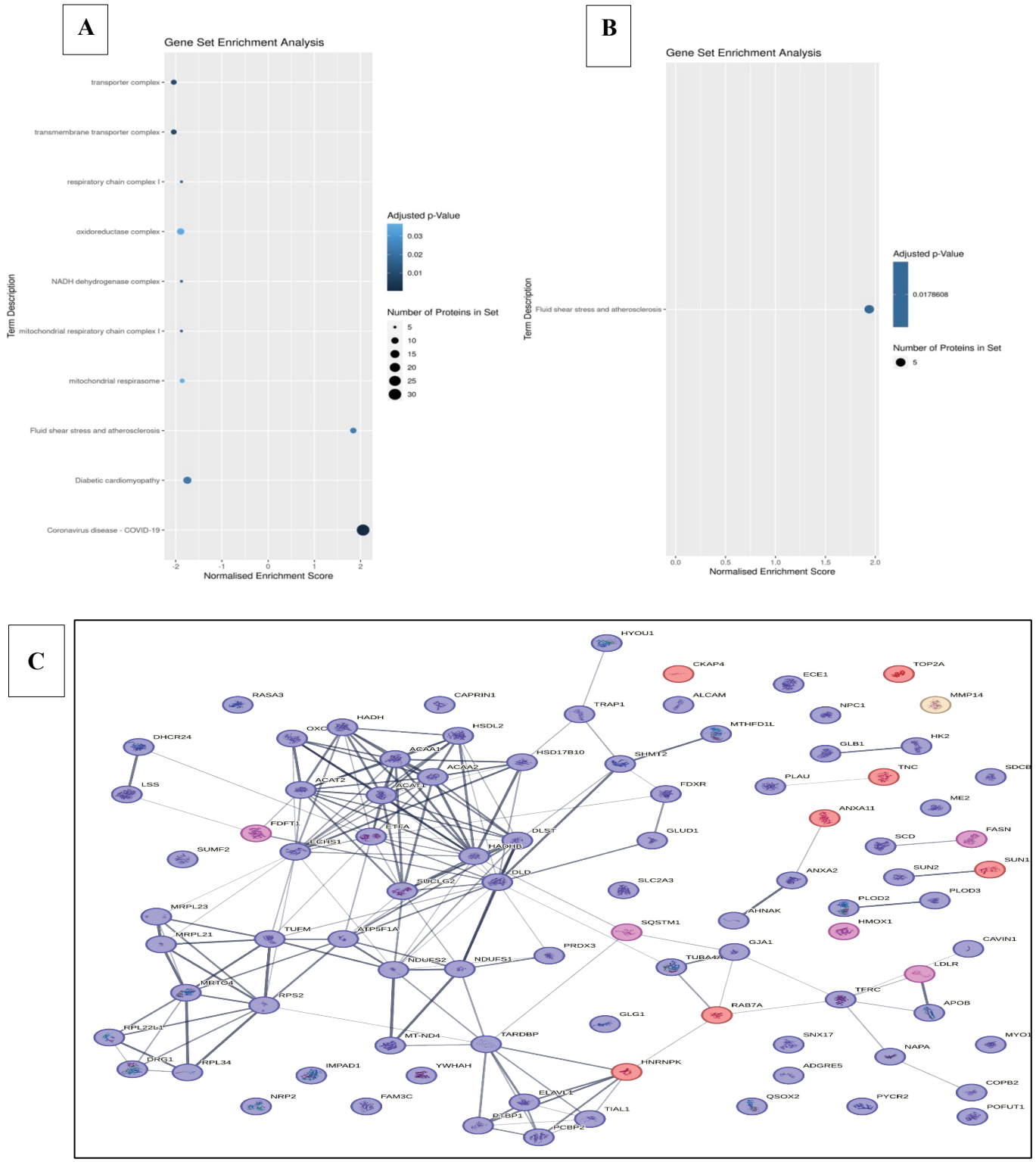

Figure 5. Enrichment Pathway Analysis of the significantly dysregulated proteins. A. In U87 cell line. B. In U373 cell line. C. Protein-protein interaction network analysis of significantly dysregulated proteins in U87 and U373 glioblastoma cell lines following amlodipine treatment. Blue nodes represent proteins uniquely dysregulated in U87, red nodes indicate proteins uniquely dysregulated in U373, and pink nodes denote proteins commonly dysregulated in both cell lines.

Table 1. Significantly dysregulated proteins enriched in the specified biological process in U373 and U87 cell lines

Gene Name	Uniprot ID	Protein Name	Regulation	Biological Process	Involvement in GBM or other cancers
Dysregulated proteins in U373 Cell line					
SQSTM1	Q13501	Sequestosome-1	Up	Regulates activation of the nuclear factor kappa-B (NF-kb) signaling pathway[27]	Cytoplasmic p62 enhances the migration and invasion abilities of esophageal cancer cells [27]
HMOX1	P09601	Heme oxygenase 1	Up	Essential enzyme in heme catabolism[28]	Inhibition of NRF2 or HO-1 enhances the sensitivity of OSCC cells to DSF/Cu-induced ferroptosis [28].
Dysregulated proteins in U87 Cell line					
NDUFS2	O75306	NADH dehydrogenase [ubiquinone] iron-sulfur protein 2, mitochondrial	Down	Complex I protein NDUFS2 is vital for growth, ROS generation, membrane integrity, apoptosis, and mitochondrial energetics.[29]	NUDT21 stabilizes NDUFS2 and activates the PI3K-AKT signaling pathway. Overexpression of NUDT21 enhances pancreatic adenocarcinoma cells proliferation and migration [29].
NDUFS1	P28331	NADH-ubiquinone oxidoreductase 75 kDa subunit, mitochondrial	Down	Involved in the oxidative phosphorylation[30]	NDUFS1 is PHB2 binding partner. Upregulation of PHB2 causes cell proliferation in colorectal cancer [30].
MT-ND4	P03905	NADH-ubiquinone oxidoreductase chain 4.	Down	Essential for the catalytic activity and assembly of complex I[31]	Mutations in MT-ND4 is associated with breast cancer [31].
DLST	P36957	Dihydrolipoyllysine-residue succinyltransferase component of 2-oxoglutarate dehydrogenase complex, mitochondrial	Down	Dihydrolipoamide succinyltransferase (DLST) is a subunit enzyme of the alpha-ketoglutarate dehydrogenase complex of the Krebs cycle	DLST loss significantly suppressed NADH production and impaired OXPHOS, leads to growth arrest and apoptosis of neuroblastoma cells.
GJA1	P17302	Gap junction alpha-1 protein	Up	A component of gap junctions, which are composed of arrays of intercellular channels that provide a route for the diffusion of low molecular weight materials from cell to cell	Gap junction protein connexin 43 (Cx43) renders GBM cells resistant to TMZ through its carboxyl terminus (CT).
NPC1	O15118	Niemann-Pick C1 protein	Up	Intracellular cholesterol transporter which acts in concert with NPC2 and plays an important role in the egress of cholesterol from the endosomal/ lysosomal compartment[32]	NPC1 is highly expressed in HCC cells and tumor tissues, which promotes the proliferation, migration, and invasion of tumor cells by activating autophagy [32].
ATP5A1	P25705	ATP synthase subunit alpha, mitochondrial	Down	produces ATP from ADP in the presence of a proton gradient	It's upregulated in metastatic lung adenocarcinoma
RPL34	P49207	60S ribosomal protein L34	Up	Catalyzes protein synthesis,	Knockdown of RPL34 inhibits the proliferation and migration of glioma cells through the inactivation of JAK/STAT3 signaling pathway
RPS2	P15880	40S ribosomal protein S2	Up	Catalyzes protein synthesis,	RPS2 mRNA expression is significantly elevated, and its promoter is hypomethylated in HCC patient samples compared to controls
DRG1	Q9Y295	Developmentally regulated GTP-binding protein 1	Down	Involved in positive regulation of microtubule polymerization and regulation of mitotic spindle assembly	DFRP1 is also overexpressed in acute myeloid leukaemia (AML), hepatocellular carcinomas, melanoma, , and osteosarcoma.
SDCBP	O00560	Syntenin-1	Up	This protein may also affect cytoskeletal-membrane organization, cell adhesion, protein trafficking, and the activation of transcription factors.	Downregulation of SDCBP inhibits cell proliferation and induces apoptosis by regulating PI3K/AKT/ mTOR pathway in gastric carcinoma.

a process known for its cancer-suppressive properties, as well as the generation of reactive oxygen species (ROS), apoptosis, and necrosis[42]. Our results also demonstrated a 1.4-fold reduction in NDUFS2 expression in amlodipine-treated cells, further indicating that amlodipine interferes with mitochondrial respiration and energy metabolism in glioma cells.

In addition to its impact on NDUFS1 and NDUFS2, amlodipine significantly downregulated MT-ND4 expression by 8.45-fold, highlighting its potential role in disrupting mitochondrial function and energy metabolism in GBM cells. MT-ND4 (NADH-ubiquinone oxidoreductase chain 4) is an essential subunit of mitochondrial complex I, responsible for electron transfer within the respiratory chain, ultimately driving ATP production. Dysregulation of MT-ND4 has been implicated in multiple cancer types, with accumulating evidence linking its mutations to cancer progression and therapy resistance. Notably, MT-ND4 mutations have been associated with cisplatin resistance, impacting chemotherapy response and overall treatment efficacy[36]. This resistance is thought to be mediated by alterations in mitochondrial membrane potential, leading to changes in oxidative phosphorylation efficiency and reduced drug-induced apoptosis. Given that amlodipine has been shown to downregulate MT-ND4 expression, it may be worth exploring whether combining amlodipine with cisplatin could help overcome cisplatin resistance by disrupting mitochondrial homeostasis and enhancing apoptosis in resistant cancer cells.

Beyond its role in chemoresistance, MT-ND4 dysregulation has been explored as a potential biomarker for cancer detection and progression, particularly in breast cancer, where its mutations correlate with disease severity[31]. In GBM, alterations in MT-ND4 expression could similarly contribute to metabolic reprogramming, promoting cancer cell survival under hypoxic conditions by modulating energy metabolism[43]. The substantial downregulation of MT-ND4 observed in U87 cells following amlodipine treatment suggests that amlodipine as an L-type VGCC blocker interferes with mitochondrial dynamics, possibly shifting GBM cells toward a less energy-efficient state. This disruption could impair cancer growth, making MT-ND4 a compelling therapeutic target for GBM treatment. Furthermore, the ability of amlodipine to reduce MT-ND4 expression highlights its potential as a repurposed therapeutic agent for GBM. Given the financial burden and limited success of novel drug development, targeting mitochondrial dysfunction using FDA-approved drugs offers a practical approach to enhancing treatment efficacy. Investigating amlodipine in combination with existing chemotherapeutic agents could provide an opportunity to overcome therapy resistance and improve patient outcomes at a lower cost.

In U373 cell line, our analysis revealed that the fluid shear stress and atherosclerosis pathway was significantly activated. Fluid shear stress refers to the frictional force exerted by fluid flow on cells and tissues. The human body consists of approximately 70% water, classified into extracellular fluid, intracellular fluid, and interstitial fluid, all of which contribute to shear stress. This mechanical force influences various cellular behaviors, including adhesion, proliferation, and differentiation[44]. Cancer progression is often accompanied by low fluid shear stress, which has been shown to play a vital role in regulating matrix metalloproteinases (MMPs). MMPs are calcium-dependent zinc-containing endoproteinases responsible for breaking down proteins in the extracellular matrix (ECM), thereby facilitating cancer invasion and metastasis[45]. Depending on the cancer's location and the specific MMPs involved, these enzymes can exert both pro-tumorigenic and anti-tumorigenic effects.

In brain cancers, key MMPs such as MMP-2, MMP-3, MMP-9, and MMP-14 are major contributors to GBM progression. MMP-2, in particular, enhances GBM metastasis and invasiveness by degrading the ECM to enable neovascularization and angiogenesis[46]. Furthermore, overexpression of MMP1, MMP3, MMP13, and TIMP1 has been identified as a critical factor in gliomagenesis, reinforcing the importance of MMP regulation in GBM pathology[47]. One of the key proteins associated with the Fluid Shear Stress pathway is Sequestosome-1 (SQSTM1/p62), an adaptor protein with diverse cellular functions, including protein degradation, autophagy regulation, and maintenance of genetic stability. SQSTM1/p62 exhibits dual functionality, participating in both cancer-suppressing and cancer-promoting pathways, particularly those associated with epithelial-mesenchymal transition (EMT) and metabolic adaptation[48]. In GBM and neuroblastoma, SQSTM1/p62 overexpression has been associated with NRF2-mediated activation of macroautophagy and mitochondrial autophagy, allowing cancer cells to evade apoptosis and develop resistance to proteasome inhibitors. Conversely, SQSTM1/p62 knockout has been shown to promote apoptosis and suppress cancer survival[49].

Our results revealed that amlodipine treatment led to a substantial upregulation of SQSTM1/p62 expression, with a 4.7-fold increase in U87 cells and a 2.9-fold increase in U373 cells. This suggests that calcium influx inhibition may modulate SQSTM1/p62-related pathways, thereby decreasing GBM progression. The differential responses observed between U87 and U373 cells underscore the heterogeneity of GBM and highlight the complex interplay between calcium signalling, fluid shear stress, and cancer-associated proteolytic pathways. Understanding these molecular alterations may offer new therapeutic insights for targeting GBM, particularly in the context of drug repurposing strategies.

From a pharmacy practice perspective, the identification of dysregulated proteins such as MT-ND4, NDUFS1, NDUFS2, and SQSTM1/p62 in GBM cell lines has significant implications for personalized medicine and therapeutic drug monitoring. These biomarkers can aid clinical pharmacists in developing patient-specific treatment strategies, particularly in optimizing the use of calcium channel blockers like amlodipine as potential adjunct therapies. Moreover, the modulation of mitochondrial function and proteolytic pathways by amlodipine opens new avenues for therapeutic drug management, including monitoring mitochondrial biomarkers to assess drug efficacy and side effects. Incorporating these molecular insights into pharmacy practice can facilitate better therapeutic outcomes by guiding drug selection, predicting response, and minimizing

adverse effects, thereby reinforcing the clinical pharmacist's role in precision oncology and enhancing the multidisciplinary care of GBM patients.

Despite these promising findings, it is important to acknowledge that this study was conducted exclusively *in vitro* using GBM cell lines. While cell-based models provide valuable insights into molecular mechanisms, they do not fully replicate the complexity of the cancer microenvironment *in vivo*. Future research should incorporate *in vivo* studies, such as xenograft mouse model, to validate these findings and assess the therapeutic potential of amlodipine in a physiologically relevant setting. Additionally, investigating the long-term effects of calcium channel inhibition on GBM progression and resistance mechanisms will be essential for translating these results into clinical applications.

CONCLUSION

This study highlights the potential of amlodipine, a calcium channel blocker, as a repurposed therapeutic agent for GBM. Proteomic analysis identified a total of 77 significantly dysregulated proteins in U87 and 14 in U373 cell lines, demonstrating that amlodipine modulates key pathways involved in mitochondrial function and fluid shear stress. In U87 cells, mitochondrial-related pathways, including oxidative phosphorylation and NADH dehydrogenase complex, were predominantly deactivated, with a notable reduction in NDUFS1, NDUFS2, and MT-ND4 expression. In contrast, U373 cells exhibited activation of the Fluid Shear Stress and Atherosclerosis pathway, with upregulation of SQSTM1/p62, suggesting a role in ECM remodelling and affecting GBM progression. These findings provide valuable insights into the molecular effects of calcium influx inhibition in GBM and support further exploration of amlodipine as a cost-effective therapeutic strategy.

AUTHOR CONTRIBUTIONS

Conceptualization and study design, M. H. S., and K. H. A., Methodology, M. H. S., R. A. Z., A. M. S., Z. A. W., M. A. Y. A., and A. M. A., Analysis and interpretation of data, M. H. S., R. A. Z., and Z. A. W., Writing original draft preparation, Z. A. W., and R. A. Z., Writing, review and editing, Z. A. W., R. A. Z., A. M. S., M. A. Y. A., A. Y. A., A. M. A., H. M. A., E. A. G., S. M. A., Z. M. A., Y. B., W. E. H., K. H. A., and M. H. S.

CONFLICTS OF INTEREST

The authors declare that they have no conflicts of interest or financial disclosures.

References

1. Rock K, Mcardle O, Forde P, Dunne M, Fitzpatrick D, O'Neill B, et al. A clinical review of treatment outcomes in glioblastoma multiforme—the validation in a non-trial population of the results of a randomised Phase III clinical trial: has a more radical approach improved survival? British Journal of Radiology. 2014;85(1017):e729-e33.
2. Hanif F, Muzaffar K, Perveen k, Malhi SM, Simjee SU. Glioblastoma Multiforme: A Review of its Epidemiology and Pathogenesis through Clinical Presentation and Treatment. Asian Pacific Journal of Cancer Prevention. 2017;18(1):3-9.
3. Ostrom QT, Gittleman H, Liao P, Rouse C, Chen Y, Dowling J, et al. CBTRUS Statistical Report: Primary Brain and Central Nervous System Tumors Diagnosed in the United States in 2007–2011. Neuro-Oncology. 2014;16(suppl_4):iv1-iv63.
4. Shergalis A, Bankhead A, Luesakul U, Muangsin N, Neamati N. Current Challenges and Opportunities in Treating Glioblastoma. Pharmacological Reviews. 2018;70(3):412-45.
5. Rapp M, Baernreuther J, Turowski B, Steiger H-J, Sabel M, Kamp MA. Recurrence Pattern Analysis of Primary Glioblastoma. World Neurosurgery. 2017;103:733-40.
6. Karim R, Palazzo C, Evrard B, Piel G. Nanocarriers for the treatment of glioblastoma multiforme: Current state-of-the-art. Journal of Controlled Release. 2016;227:23-37.
7. Munoz JL, Walker ND, Scotto KW, Rameshwar P. Temozolomide competes for P-glycoprotein and contributes to chemoresistance in glioblastoma cells. Cancer Letters. 2015;367(1):69-75.
8. Soeda A, Hara A, Kunisada T, Yoshimura S-i, Iwama T, Park DM. The Evidence of Glioblastoma Heterogeneity. Scientific Reports. 2015;5(1):7979.
9. Field KM, Jordan JT, Wen PY, Rosenthal MA, Reardon DA. Bevacizumab and glioblastoma: Scientific review, newly reported updates, and ongoing controversies. Cancer. 2015;121(7):997-1007.
10. Haque A, Banik NL, Ray SK. Molecular alterations in glioblastoma: potential targets for immunotherapy. Prog Mol Biol Transl Sci. 2011;98:187-234.
11. Esemen Y, Awan M, Parwez R, Baig A, Rahman S, Masala I, et al. Molecular Pathogenesis of Glioblastoma in Adults and Future Perspectives: A Systematic Review. International Journal of Molecular Sciences. 2022;23(5):2607.
12. Aly A, Singh P, Korytowsky B, Ling Y-L, Kale HP, Dastani HB, et al. Survival, costs, and health care resource use by line of therapy in US Medicare patients with newly diagnosed glioblastoma: a retrospective observational study. Neuro-Oncology Practice. 2019;7(2):164-75.
13. Ohgaki H, Kleihues P. Population-Based Studies on Incidence, Survival Rates, and Genetic Alterations in Astrocytic and Oligodendroglial Gliomas. Journal of Neuropathology & Experimental Neurology. 2005;64(6):479-89.

14. Basso J, Miranda A, Sousa J, Pais A, Vitorino C. Repurposing drugs for glioblastoma: From bench to bedside. Cancer Letters. 2018;428:173-83.
15. Elliott WJ, Ram CV. Calcium channel blockers. J Clin Hypertens (Greenwich). 2011;13(9):687-9.
16. Alqudah MA, Yaseen MM, Alzoubi KH, Al-Husein BA, Bardaweel SK, Abuhelwa AY, et al. Metabolomic Analysis, Antiproliferative, Anti-Migratory, and Anti-Invasive Potential of Amlodipine in Lung Cancer Cells. 2025:1215-29.
17. Alqudah MAY, Al-Samman R, Azaizeh M, Alzoubi KH. Amlodipine inhibits proliferation, invasion, and colony formation of breast cancer cells. Biomed Rep. 2022;16(6):50.
18. Mohammad A.Y. Alqudah a b, *, RA-Sb, KHA. The interactive effect of amlodipine and chemotherapeutic agents in lung cancer cells Informatics in Medicine Unlocked 2022.
19. Fu B, Dou X, Zou M, Lu H, Wang K, Liu Q, et al. Anticancer Effects of Amlodipine Alone or in Combination With Gefitinib in Non-Small Cell Lung Cancer. Front Pharmacol. 2022;13:902305.
20. Hassanein MM, Hagyousif YA, Zenati RA, Al-Hroub HM, Khan FM, Abuhelwa AY, et al. Metabolomics insights into doxorubicin and 5-fluorouracil combination therapy in triple-negative breast cancer: a xenograft mouse model study. 2025;11:1517289.
21. Abufares HI, Zenati RA, Soares NC, El-Huneidi W, Dahabiyeh LA, Al-Hroub HM, et al. A non-targeted metabolomics comparative study on plasma of pfizer and sinopharm COVID-19 vaccinated individuals, assessed by (TIMS-QTOF) mass spectrometry. 2024;10(15).
22. Heo YJ, Hwa C, Lee G-H, Park J-M, An J-YJM, cells. Integrative multi-omics approaches in cancer research: from biological networks to clinical subtypes. 2021;44(7):433-43.
23. Abufares HI, Oyoun Alsoud L, Alqudah MA, Shara M, Soares NC, Alzoubi KH, et al. COVID-19 vaccines, effectiveness, and immune responses. 2022;23(23):15415.
24. Al-Amrani S, Al-Jabri Z, Al-Zaabi A, Alshekaili J, Al-Khabori MJWjobc. Proteomics: Concepts and applications in human medicine. 2021;12(5):57.
25. Motaln H, Koren A, Gruden K, Ramšak Ž, Schichor C, Lah TT. Heterogeneous glioblastoma cell cross-talk promotes phenotype alterations and enhanced drug resistance. Oncotarget. 2015;6(38):40998-1017.
26. Zenati RA, Giddey AD, Al-Hroub HM, Hagyousif YA, El-Huneidi W, Bustanji Y, et al. Evaluation of two simultaneous metabolomic and proteomic extraction protocols assessed by ultra-high-performance liquid chromatography tandem mass spectrometry. 2023;24(2):1354.
27. Liu Z, Yang LY, Hao JJ, Zhang N, Fan ZL, Cai HQ, et al. Nuclear-cytoplasmic translocation of SQSTM1/p62 protein enhances ESCC cell migration and invasion by stabilizing EPLIN expression. Exp Cell Res. 2024;435(1):113910.
28. Zhao Y, Zhu S. Nrf2/HO-1 Alleviates Disulfiram/Copper-Induced Ferroptosis in Oral Squamous Cell Carcinoma. Biochem Genet. 2024;62(1):144-55.
29. Bandara AB, Drake JC, James CC, Smyth JW, Brown DA. Complex I protein NDUFS2 is vital for growth, ROS generation, membrane integrity, apoptosis, and mitochondrial energetics. Mitochondrion. 2021;58:160-8.
30. Ren L, Meng L, Gao J, Lu M, Guo C, Li Y, et al. PHB2 promotes colorectal cancer cell proliferation and tumorigenesis through NDUFS1-mediated oxidative phosphorylation. Cell Death & Disease. 2023;14(1):44.
31. Arezi P, Rezvani Z. The variation of mitochondrial NADH dehydrogenase subunit 4 (mtND4) and molecular dynamics simulation of SNPs among Iranian women with breast cancer. Journal of Molecular Graphics and Modelling. 2018;85:242-9.
32. Xu J, Chen F, Zhu W, Zhang W. NPC1 promotes autophagy with tumor promotion and acts as a prognostic model for hepatocellular carcinoma. Gene. 2024;897:148050.
33. Monteith GR, Prevarskaya N, Roberts-Thomson SJ. The calcium–cancer signalling nexus. Nature Reviews Cancer. 2017;17(6):373-80.
34. Piste P, Sayaji D, Avinash M. Calcium and its Role in Human Body. Int J Res Pharm Biomed Sci. 2012;4:2229-3701.
35. Azab MA, Alomari A, Azzam AY. Featuring how calcium channels and calmodulin affect glioblastoma behavior. A review article. Cancer Treatment and Research Communications. 2020;25:100255.
36. Van Gisbergen M, Voets A, Starmans M, Coo F, Yadak R, Hoffmann R, et al. How do changes in the mtDNA and mitochondrial dysfunction influence cancer and cancer therapy? Challenges, opportunities and models. Mutation Research/Reviews in Mutation Research. 2015;290.
37. Boyman L, Karbowski M, Lederer WJ. Regulation of Mitochondrial ATP Production: Ca(2+) Signaling and Quality Control. Trends Mol Med. 2020;26(1):21-39.
38. Matlin KS. The Heuristic of Form: Mitochondrial Morphology and the Explanation of Oxidative Phosphorylation. J Hist Biol. 2016;49(1):37-94.
39. Huang X-D, Chen Y-W, Tian L, Du L, Cheng X-C, Lu Y-X, et al. NUDT21 interacts with NDUFS2 to activate the PI3K/AKT pathway and promotes pancreatic cancer pathogenesis. 2024;150(1):8.
40. Huang X-D, Chen Y-W, Tian L, Du L, Cheng X-C, Lu Y-X, et al. NUDT21 interacts with NDUFS2 to activate the PI3K/AKT pathway and promotes pancreatic cancer pathogenesis. Journal of Cancer Research and Clinical Oncology. 2024;150(1):8.
41. Zickermann V, Wirth C, Nasiri H, Siegmund K, Schwalbe H, Hunte C, et al. Structural biology. Mechanistic insight from the crystal structure of mitochondrial complex I. Science. 2015;347(6217):44-9.
42. Iverson TM, Singh PK, Cecchini G. An evolving view of complex II-noncanonical complexes, megacomplexes, respiration,

signaling, and beyond. J Biol Chem. 2023;299(6):104761.
43. Xu Y, Xue D, Kyani A, Bankhead III A, Roy J, Ljungman M, et al. First-in-Class NADH/Ubiquinone Oxidoreductase Core Subunit S7 (NDUFS7) antagonist for the treatment of pancreatic Cancer. 2023;6(8):1164-81.
44. Espina JA, Cordeiro MH, Milivojevic M, Pajić-Lijaković I, Barriga EH. Response of cells and tissues to shear stress. Journal of Cell Science. 2023;136(18).
45. Cabral-Pacheco GA, Garza-Veloz I, Castruita-De la Rosa C, Ramirez-Acuña JM, Perez-Romero BA, Guerrero-Rodriguez JF, et al. The Roles of Matrix Metalloproteinases and Their Inhibitors in Human Diseases. International Journal of Molecular Sciences. 2020;21(24):9739.
46. Qazi H, Shi Z-D, Tarbell JM. Fluid Shear Stress Regulates the Invasive Potential of Glioma Cells via Modulation of Migratory Activity and Matrix Metalloproteinase Expression. PLOS ONE. 2011;6(5):e20348.
47. Dibdiakova K, Majercikova Z, Galanda T, Richterova R, Kolarovszki B, Racay P, et al. Relationship between the Expression of Matrix Metalloproteinases and Their Tissue Inhibitors in Patients with Brain Tumors. International Journal of Molecular Sciences. 2024;25(5):2858.
48. Tang J, Li Y, Xia S, Li J, Yang Q, Ding K, et al. Sequestosome 1/p62: A multitasker in the regulation of malignant tumor aggression. 2021;59(4):77.
49. Tang J, Li Y, Xia S, Li J, Yang Q, Ding K, et al. Sequestosome 1/p62: A multitasker in the regulation of malignant tumor aggression (Review). Int J Oncol. 2021;59(4):77.

https://doi.org/10.18549/PharmPract.2026.1.3357

Table S1. Significantly Dysregulated Proteins in U87 and U373 Cell Lines Following Amlodipine Treatment

Gene Name	Uniprot ID	Protein Name	Regulation	Biological Process
Dysregulated proteins in U373 Cell line				
H0Y6N5	SUN1	SUN domain-containing protein 1	0.0356	-5.261398529
P11388	TOP2A	DNA topoisomerase 2-alpha	0.029333333	-2.022019329
P50995	ANXA11	Annexin A11	0.014	-1.569287833
A0A0S2Z377	ANXA6	Annexin A6;Annexin	0.0128	-1.47057873
P61978	HNRNPK	Heterogeneous nuclear ribonucleoprotein K	0.05	-1.241263886
Q07065	CKAP4	Cytoskeleton-associated protein 4	0.042461538	1.198693051
P51149	RAB7A	Ras-related protein Rab-7a	0.036727273	1.22738235
P24821	TNC	Tenascin	0.033	1.332571484
A0A0U1RQF0	FASN	Fatty acid synthase	0.036333333	1.399594599
O60462	NRP2	Neuropilin-2	0.013333333	1.474932682
P09601	HMOX1	Heme oxygenase 1	0.018285714	2.401794515
J3KMZ9	LDLR	Low-density lipoprotein receptor	0.014	2.567143161
Q13501	SQSTM1	Sequestosome-1	0.012	2.967311123
P37268	FDFT1	Squalene synthase	0.012666667	3.243640302
Dysregulated proteins in U87 Cell line				
P03905	MT-ND4	NADH-ubiquinone oxidoreductase chain 4	0.016571429	-8.451313789
A0A3B3ISF9	ECE1	Endothelin-converting enzyme 1	0.0024	-2.18726614
Q9NX62	IMPAD1	Inositol monophosphatase 3	0.012695652	-1.980431839
E7ET40	PLAU	Urokinase-type plasminogen activator;Urokinase-type plasminogen activator long chain A;Urokinase-type plasminogen activator short chain A;Urokinase-type plasminogen activator chain B	0.036129032	-1.79469033
Q13740	ALCAM	CD166 antigen	0.026222222	-1.759803911
Q6ZRP7	QSOX2	Sulfhydryl oxidase 2	0.03880597	-1.753298875
P48960	CD97	CD97 antigen;CD97 antigen subunit alpha;CD97 antigen subunit beta	0.02427907	-1.605050243
Q7Z2W9	MRPL21	39S ribosomal protein L21, mitochondrial	0.0035	-1.590386472
Q92896	GLG1	Golgi apparatus protein 1	0.00825	-1.570444566
Q6YN16	HSDL2	Hydroxysteroid dehydrogenase-like protein 2	0.006769231	-1.515742283
Q9Y295	DRG1	Developmentally-regulated GTP-binding protein 1	0.035285714	-1.470137978
A0A087WVM4	MTHFD1L	Monofunctional C1-tetrahydrofolate synthase, mitochondrial	0.013272727	-1.45331688
C9JYQ9	RPL22L1	60S ribosomal protein L22-like 1	0.034588235	-1.447068664
F5H6E2	MYO1C	Unconventional myosin-Ic	0.0384	-1.439048108
P30084	ECHS1	Enoyl-CoA hydratase, mitochondrial	0.041315068	-1.438843664
E9PF18	HADH	Hydroxyacyl-coenzyme A dehydrogenase, mitochondrial	0.009111111	-1.420685126
J3KQJ1	SUMF2	Sulfatase-modifying factor 2	0.0415	-1.411103448
A0A087WTV6	PYCR2	Pyrroline-5-carboxylate reductase 2	0.0126	-1.406819188
Q92520	FAM3C	Protein FAM3C	0.033509434	-1.402186276
H7C2P7	MRPL23	39S ribosomal protein L23, mitochondrial	0.024857143	-1.390188492
P28331	NDUFS1	NADH-ubiquinone oxidoreductase 75 kDa subunit, mitochondrial	0.02	-1.361892273
Q13148	TARDBP	TAR DNA-binding protein 43	0.007466667	-1.361698791
P30048	PRDX3	Thioredoxin-dependent peroxide reductase, mitochondrial	0.029083333	-1.350800086
Q09666	AHNAK	Neuroblast differentiation-associated protein AHNAK	0.002285714	-1.345126995
P13804	ETFA	Electron transfer flavoprotein subunit alpha, mitochondrial	0.01716129	-1.34508965
Q9UH99	SUN2	SUN domain-containing protein 2	0.028653061	-1.345082537

www.pharmacypractice.org (eISSN: 1886-3655 ISSN: 1885-642X)

Q01085	TIAL1	Nucleolysin TIAR	0.0246	-1.342066847
P34897	SHMT2	Serine hydroxymethyltransferase, mitochondrial	0.006545455	-1.340349527
P68366	TUBA4A	Tubulin alpha-4A chain	0.0370625	-1.33972184
P55809	OXCT1	Succinyl-CoA:3-ketoacid coenzyme A transferase 1, mitochondrial	0.010947368	-1.338840835
O75306	NDUFS2	NADH dehydrogenase [ubiquinone] iron-sulfur protein 2, mitochondrial	0.048266667	-1.337426607
Q12931	TRAP1	Heat shock protein 75 kDa, mitochondrial	0.02	-1.315460816
Q9H488	POFUT1	GDP-fucose protein O-fucosyltransferase 1	0.003111111	-1.312597436
A0A1W2PQT3	ME2	NAD-dependent malic enzyme, mitochondrial	0.01616	-1.290621611
Q99714	HSD17B10	3-hydroxyacyl-CoA dehydrogenase type-2	0.02	-1.288598394
P24752	ACAT1	Acetyl-CoA acetyltransferase, mitochondrial	0.008	-1.287779893
Q9UKD2	MRTO4	mRNA turnover protein 4 homolog	0.018424242	-1.287210917
P26599	PTBP1	Polypyrimidine tract-binding protein 1	0.024545455	-1.275133115
P16278	GLB1	Beta-galactosidase	0.03579661	-1.271956331
O60568	PLOD3	Procollagen-lysine,2-oxoglutarate 5-dioxygenase 3	0.017655172	-1.2718486
P36957	DLST	Dihydrolipoyllysine-residue succinyltransferase component of 2-oxoglutarate dehydrogenase complex, mitochondrial	0.027652174	-1.269517242
A0A7I2V5T4	ACO2	Aconitate hydratase, mitochondrial	0.027829787	-1.269018576
Q14444	CAPRIN1	Caprin-1	0.037818182	-1.259843597
Q96I99	SUCLG2	Succinyl-CoA ligase [GDP-forming] subunit beta, mitochondrial	0.038764706	-1.250013215
P49411	TUFM	Elongation factor Tu, mitochondrial	0.035854545	-1.238020455
P00367	GLUD1	Glutamate dehydrogenase 1, mitochondrial;Glutamate dehydrogenase 2, mitochondrial	0.016592593	-1.228156021
A0A087X054	HYOU1	Hypoxia up-regulated protein 1	0.048623377	-1.228061687
Q14644	RASA3	Ras GTPase-activating protein 3	0.025463415	-1.227267415
Q6NZI2	PTRF	Polymerase I and transcript release factor	0.048842105	-1.225996112
P07355	ANXA2	Annexin A2	0.02928	-1.218158496
A0A0A0MTN9	FDXR	NADPH:adrenodoxin oxidoreductase, mitochondrial	0.040285714	-1.21801195
E7ETU9	PLOD2	Procollagen-lysine	0.036148148	-1.207587975
P02786	TFRC	Transferrin receptor protein 1;Transferrin receptor protein 1, serum form	0.015846154	-1.197056161
P25705	ATP5A1	ATP synthase subunit alpha, mitochondrial	0.019487179	-1.196639273
M0R0Y2	NAPA	Alpha-soluble NSF attachment protein	0.035266667	-1.192855584
Q15366	PCBP2	Poly(rC)-binding protein 2	0.035606557	-1.162684406
Q15717	ELAVL1	ELAV-like protein 1	0.012190476	-1.144411442
P15880	RPS2	40S ribosomal protein S2	0.041577465	1.165679251
H0Y938	COPB2	Coatomer subunit beta	0.035103448	1.354817917
O15118	NPC1	Niemann-Pick C1 protein	0.007333333	1.374701812
P48449	LSS	Lanosterol synthase	0.021028571	1.384086758
Q04917	YWHAH	14-3-3 protein eta	0.040637681	1.458085511
P50281	MMP14	Matrix metalloproteinase-14	0.0036	1.466926015
O00560	SDCBP	Syntenin-1	0.020444444	1.493947656
P17302	GJA1	Gap junction alpha-1 protein	0.017066667	1.514839518
P52789	HK2	Hexokinase-2	0.019	1.815988134
A0A0A0MTI1	DHCR24	Delta(24)-sterol reductase	0.037015873	1.845590654
J3KMZ9	LDLR	Low-density lipoprotein receptor	0.007714286	1.906180736
P49207	RPL34	60S ribosomal protein L34	0.041081081	1.916430436
E9PNM1	FDFT1	Squalene synthase	0.03522807	2.245275431

P09601	HMOX1	Heme oxygenase 1	0	2.390718374
A0A0U1RQF0	FASN	Fatty acid synthase	0.002	2.631302647
Q15036	SNX17	Sorting nexin-17	0.034076923	2.675793342
P04114	APOB	Apolipoprotein B-	0	3.574253684
P11169	SLC2A3	Solute carrier family 2	0.016833333	3.703200296
Q13501	SQSTM1	Sequestosome-1	0	4.713072336
O00767	SCD	Acyl-CoA desaturase	0	8.269591254

www.pharmacypractice.org (eISSN: 1886-3655 ISSN: 1885-642X)